Design storm duration from hourly rainfall records in a bimodal Andean climate

Integrating WMO-168 data screening, cascade infilling, and IETD-based frequency analysis for the CVC hydrometeorological network, Valle del Cauca, Colombia

Mauricio Javier Victoria Niño[1]

[1]Independent Researcher, Cali, Colombia; hidratecsa@gmail.com; ORCID: 0009-0003-4328-5691

Version 2. *This revised version incorporates the coefficient of advance (r) analysis for synthetic hyetograph construction (Sections 2.5, 3.4, 4.3, Table 3, Figure 11). The original version (v1) was posted on May 15, 2026.*

This document is a preprint that has not been peer-reviewed, submitted to EngrXiv. Supplementary implementation code and case-study data are available at: https://github.com/MauricioVictoriaN/DesignStormDuration-CVC. Case study: La Primavera station, Guadalajara de Buga municipality, Valle del Cauca — CVC hydrometeorological network.

Abstract

Context and motivation. Hydrological design in convective tropical regions requires a reliable estimate of the design storm duration: the continuous rainfall time that feeds rainfall-runoff transformation models for a given return period. In the Valle del Cauca (Colombia), the Corporación Autónoma Regional del Valle del Cauca (CVC) hydrometeorological network provides hourly pluviographic records, but their direct use for design is hampered by three systematic obstacles: (i) a proprietary block-monthly storage format with mixed missing-data codes; (ii) structural data availability capped at 64–67 % because the dataloggers operate on a variable duty cycle (typically 8–16 active hours per day depending on acquisition mode); and (iii) the absence of a standardised quality-control and frequency-analysis protocol adapted to the bimodal Andean climate.

Objective. To present and validate a complete methodological framework for processing hourly rainfall series of the CVC network, from raw data screening through the probabilistic estimation of design storm durations for return periods of 2–200 years, including the systematic derivation of the coefficient of advance (r) — the temporal position of the intensity peak within each storm — applied to La Primavera station (Guadalajara de Buga, 1 644 m a.s.l., 1970–2025).

Methods. The framework integrates five complementary stages: (i) quality control and cascade infilling (piecewise linear interpolation for gaps ≤ 6 h; hourly climatology by month for longer gaps, following Paulhus & Kohler [9] for the climatological stage only); (ii) annual screening against WMO-No. 168 Criteria C1–C2 [15], adapted to the structural availability of CVC dataloggers; (iii) identification of independent storm events through the Inter-Event Time Definition

(IETD) criterion of Restrepo-Posada & Eagleson [12], with a physical upper bound of 6 h for Andean tropical convection [10]; (iv) frequency analysis of storm durations fitting four probability distributions (Exponential, Gamma, Log-Normal, Weibull), evaluated by the Kolmogorov-Smirnov goodness-of-fit test; and (v) derivation of the coefficient of advance $r_j = (t_{\text{pico},j} - t_{\text{inicio},j})/D_j$ for each independent storm, where D_j is the physical duration, providing the temporal asymmetry metric needed for synthetic hyetograph construction.

Results. Nine years (2016–2025, excluding 2017) pass the WMO-168 screening, yielding a mean availability of 64 %. With IETD = 6 h, 1 027 independent storms are catalogued (rate = 114 storms/yr; mean depth = 19 mm; mean physical duration = 6.6 h). The inter-event time coefficient of variation ($\mathrm{Cv}_{\mathrm{TBT}} = 4.47$) reflects bimodal seasonal clustering and confirms a non-Poisson arrival process — relevant only to the IETD-based storm definition; the subsequent frequency analysis is empirical and arrival-process-agnostic. The Log-Normal distribution ($\mu_{\ln} = 1.352$, $\sigma_{\ln} = 0.743$; $D_{\mathrm{KS}} = 0.093$, lowest among the four candidates) best describes the duration population. The coefficient of advance shows a median $r = 0.167$ (mean $= 0.248$, SD $= 0.195$), indicating that the intensity peak occurs typically in the first 17 % of the storm duration — a signature of the impulsive onset characteristic of tropical convective precipitation. Design durations are 3.86 h ($T_r = 2$ yr), 10.0 h ($T_r = 10$ yr), and 21.7 h ($T_r = 100$ yr), consistent with the regional hydrometeorological literature for the Colombian Andes.

Conclusions. The proposed framework provides a reproducible, normatively grounded procedure for deriving design storm durations and the coefficient of advance directly from the observed hourly record without requiring neighbouring-station data or regional regression models. The methodology is transferable to any CVC station by adjusting a minimal set of site-specific parameters.

Keywords: hourly rainfall; quality control; climatological infilling; WMO-168; IETD; Restrepo-Posada & Eagleson; design storm duration; coefficient of advance; Log-Normal; Valle del Cauca; Colombian Andes.

Data and code availability: The R implementation (v1.0.0) and case-study data are provided as supplementary material at https://github.com/MauricioVictoriaN/DesignStormDuration-CVC under an MIT licence.

1 Introduction

The design storm duration is the characteristic time of continuous rainfall that is used as the driving input to rainfall-runoff transformation models for sizing drainage, flood-protection, and water-supply structures [2, 15]. Unlike the design intensity, which is widely documented through intensity-duration-frequency (IDF) curves, the design *duration* is rarely derived from the observed record and is instead assumed *a priori* on the basis of engineering judgment or empirical rules [5]. This practice introduces substantial uncertainty in hydrological design, particularly in convective tropical regimes where storm durations span two orders of magnitude (1–100 h) depending on the type of meteorological system [10].

A further gap exists in the characterisation of the *temporal asymmetry* of the design storm — the coefficient of advance r, defined as the fraction of the storm duration elapsed before the peak intensity occurs [2]. This parameter is essential for constructing synthetic hyetographs (e.g., alternating-block or Huff curves) but is typically assigned a default value ($r \approx 0.3$–0.5) without site-specific validation. For tropical convective storms, where the onset is often abrupt and the recession gradual, the coefficient of advance may deviate substantially from these assumed values.

In the Valle del Cauca (Colombia), the CVC operates a hydrometeorological network of hourly tipping-bucket rain gauges. The raw data files use a proprietary block-monthly format that is not directly readable by standard tabular tools, and the dataloggers operate on a variable duty cycle (typically 8–16 active hours per day), generating a structurally incomplete series even in fault-free years, with observed annual availability capped at 64–67 %. The WMO Guide to Hydrological Practices [15] recommends an 80 % annual availability threshold before a year is admitted to frequency analysis, but this criterion indiscriminately rejects all years from CVC stations operating under this duty cycle. No published adaptation of WMO-168 to this type of datalogger is known.

The Inter-Event Time Definition (IETD) method of Restrepo-Posada & Eagleson [12] identifies independent storm events by selecting the minimum dry-period threshold that makes the inter-event time series consistent with a Poisson arrival process (coefficient of variation $\mathrm{Cv} = 1$). This criterion has been widely applied in urban hydrology [1, 4] and forms the foundation for probabilistic storm catalogues. However, its application to bimodal climates, where long inter-seasonal dry periods coexist with intra-seasonal bursts of activity, has received limited attention [4].

1.1 Research objectives

1. Develop a step-by-step methodological framework for quality control, cascade infilling, and WMO-168 annual screening of hourly rainfall series from CVC dataloggers, with normative justification for threshold adaptations.
2. Apply the IETD criterion of Restrepo-Posada & Eagleson [12] with a physically motivated upper bound for Andean tropical convection, and characterise the non-Poisson behaviour of storm arrival in the bimodal Valle del Cauca climate.
3. Fit and compare four probability distributions to the empirical population of independent storm durations — regardless of the arrival-process model — and derive design durations with explicit 95 % bootstrap confidence intervals for return periods within and beyond the observed range, with explicit validity limits based on record length.
4. Derive the coefficient of advance r for each independent storm from the ratio of the peak-occurrence time to the physical duration, and characterise its statistical distribution for use in

synthetic hyetograph construction.

5. Provide transferable guidance for applying the methodology to any CVC station.

2 Materials and Methods

2.1 Study area and data

The Valle del Cauca inter-Andean valley (Colombia, 3–5°N, 76–77°W) exhibits a bimodal rainfall regime driven by the semi-annual migration of the Intertropical Convergence Zone, with two wet seasons (March–May, September–November) and two dry seasons (June–August, December–February) [10, 5]. Convective precipitation dominates, with storm depths of 1–200 mm, typical intensities of 5–50 mm/h, and isolated maxima exceeding 100 mm/h [5]. Mean annual precipitation ranges from 1 500 to 2 500 mm in the inter-Andean plain.

La Primavera station (Guadalajara de Buga; 1 644 m a.s.l.; $\approx 3.9^{\circ}$N, 76.3°W; CVC network) was chosen as the case study because it represents the Andean-Centre hydroclimatic sub-region of the Cauca system [6] and has the longest available digital record among CVC hourly stations in the region. Table 1 summarises the station metadata and key results.

Table 1: Metadata of La Primavera station and main results of the analysis. n_{valid} = number of hourly records passing quality control.

Attribute	Value
Station name	La Primavera
Municipality	Guadalajara de Buga
Department	Valle del Cauca, Colombia
Network	CVC
Elevation	1 644 m a.s.l.
Nominal record period	1970–2025
Effective data period	2014–2025
Valid years after WMO-168 screening	9 (2016, 2018–2025)
Mean annual availability (valid years)	64.0 %
n_{valid} (hourly records)	56 384
Maximum recorded hourly intensity	123.2 mm/h
Mean annual rainfall (valid years)	2 189 mm
Month of maximum rainfall	April (88 mm/month)
Hour of maximum convective activity	15:00–16:00 local time
IETD adopted	6 h
N independent storms catalogued	1 027
Mean storm rate	114 storms/yr
Mean physical duration	6.6 h
Median coefficient of advance (r)	0.167

The raw data file supplied by CVC is an Excel workbook with a non-standard block-monthly layout: data for each month occupy a group of rows preceded by a month-year label row and a header row containing the text `DÍA\HORA` followed by the hour identifiers 00–23 in non-contiguous columns. Missing values are encoded as `***<`, `NA`, or empty cells. All analyses were implemented in R 4.3 [11]; the implementation is available as supplementary material [14].

2.2 Quality control and cascade infilling

Each hourly record is classified into one of four categories based on its numerical value and missing-data code:

1. **Valid:** $0 \leq P \leq P_{\max}$, not a missing-data code.
2. **Missing:** `***<`, `NA`, or empty cell.
3. **Negative:** $P < 0$ (instrument error).
4. **Extreme:** $P > P_{\max} = 130$ mm/h. This threshold corresponds to the upper envelope of recorded hourly intensities in the Valle del Cauca inter-Andean plain: IDEAM [5] reports absolute maxima in the 80–130 mm/h range for stations in this region, and values exceeding 130 mm/h are physically implausible for the prevailing convective mechanism and tipping-bucket resolution.

Records in categories 2–4 are imputed through a three-stage cascade:

Stage 1 — Linear interpolation. For gaps of up to $\Delta t_{\max} = 6$ h, piecewise linear interpolation between the nearest valid records before and after the gap is applied. This standard numerical method handles intra-event data dropouts where the temporal gradient of precipitation is approximately linear.

Stage 2 — Climatological infilling. For longer gaps, each missing record at hour h of month m is replaced by the long-term mean of all valid observations for the same (m, h) combination:

$$\hat{P}_{m,h} = \frac{1}{n_{m,h}} \sum_{t \in \mathcal{V}_{m,h}} P_t, \tag{1}$$

where $\mathcal{V}_{m,h} = \{t : \text{hour}(t) = h,\ \text{month}(t) = m,\ P_t \text{ valid}\}$ is the set of temporal indices corresponding to hour h of month m across all years in the record, and $n_{m,h} = |\mathcal{V}_{m,h}|$ is its cardinality [9, 13]. With 192 available (m, h) combinations, this method captures the diurnal and seasonal structure of precipitation and reduces the systematic overestimation bias introduced by local interpolation near dry-period boundaries.

Stage 3 — Zero imputation. Residual gaps without sufficient neighbours for climatological estimation are set to zero, representing the assumption of a dry period.

Cross-validation (random withdrawal of 5 % of valid records) yields Nash-Sutcliffe Efficiency (NSE) of 0.005 for the climatological infilling versus NSE $= -0.26$ for linear interpolation alone. Moriasi et al. [8] note that NSE is an unreliable discriminator for time series with a high proportion of zero or near-zero values ($\approx$ 90 % dry hours here), because the denominator $\sum(Q_{\text{obs}} - \bar{Q})^2$ is dominated by the dry-period variance and small absolute errors in rainy-hour predictions can drive the statistic strongly negative. PBIAS and RMSE are therefore the preferred skill metrics for this application: the percent bias of 22.4 % for climatological infilling versus 22.9 % for linear interpolation confirms the superiority of Stage 2 in reducing systematic bias over long gaps.

2.3 Annual data screening: WMO-168 adaptation

Section 5.4 of WMO No. 168 [15] recommends a minimum annual data availability of 80 % for admitting a year to frequency analysis. This threshold implicitly assumes continuously recording instruments. CVC dataloggers, however, operate on a variable duty cycle: the acquisition mode alternates between active periods (8–16 h/day depending on the season and configuration) and standby, generating structurally incomplete records even in fault-free years.[1] Applying the 80 % threshold unconditionally would exclude all available years, which contradicts the spirit of the guideline.

The WMO-168 §5.4 footnote explicitly permits threshold reduction for isolated stations without regional filling alternatives. The IDEAM national protocol [5] similarly allows adjusted thresholds for semi-automatic recorders. The following adapted criteria are applied:

Criterion C1 (WMO-168 §5.4): Annual availability $\geq 60\,\% \Rightarrow$ year admitted (VALID-C1).

Criterion C2 (WMO-168 §5.7): Availability in the wet season (March–May, September–November, bimodal CVC regime [10]) $\geq 50\,\%$, even if C1 is not met $\Rightarrow$ year admitted (VALID-C2).

Criterion C3 (WMO-168 §5.7): Maximum within-month gap in a wet-season month — **deactivated.** Internal monthly gaps of $\approx$30 days are structural artefacts of the datalogger duty cycle (not measurement failures) and must not invalidate a year for IETD analysis.

Only years from *ANIO_INICIO_UTIL* $= 2014$ onward are evaluated; the nominal 1970–2013 period contains zero valid records, as confirmed by the raw availability diagnostic.

2.4 Identification of independent storms (IETD)

Storm properties and inter-event time. An hour is classified as rainy if $P \geq I_{\min} = 0.1$ mm/h. A new independent storm event j is initiated when the cumulative dry period since the last rainy hour equals or exceeds the IETD threshold h. For event j, four properties are recorded: start time t_j, duration as hours with measurable rainfall D_j^{rain}, physical duration D_j (time span from first to last rainy hour plus one hour), and total depth $P_j = \sum P_t$. Events with $P_j < P_{\min} = 1.0$ mm are discarded as instrumental traces. The inter-event times between successive storm initiations are:

$$\mathrm{TBT}_k = t_{k+1} - t_k, \quad k = 1, \ldots, N-1, \tag{2}$$

where t_k is the start time of the k-th storm and N is the total number of events.

The Cv = 1 criterion and its physical interpretation. Restrepo-Posada & Eagleson [12] showed that if storm arrivals follow a stationary Poisson process, inter-event times are exponentially distributed, and therefore their coefficient of variation equals exactly unity:

$$\mathrm{Cv}_{\mathrm{TBT}}(h) = \frac{\sigma_{\mathrm{TBT}}(h)}{\mu_{\mathrm{TBT}}(h)} = 1. \tag{3}$$

The interpretation of departures from unity is physically meaningful. $\mathrm{Cv} < 1$ (under-dispersion) indicates *sub-separation*: the chosen IETD is too short and artificially fragments multi-cellular convective systems into multiple spurious events, compressing the TBT distribution and biasing

[1] The variable duty cycle explains the observed annual availability of 64–67 % (Table 1). A fixed 8-h/day cycle would imply a maximum of $8/24 \approx 33\,\%$; the higher observed values confirm that a fraction of days have continuous or extended recording, likely during wet-season active deployment periods.

duration estimates downward. $\mathrm{Cv} > 1$ (over-dispersion) indicates *over-aggregation*: the IETD is too long and merges meteorologically distinct storms — or, in bimodal climates, entire intra-season and inter-season periods — into pseudo-events that do not correspond to any real atmospheric mechanism, inflating duration estimates [1, 4]. Both biases propagate directly into the frequency-analysis quantiles and therefore into the design storm duration: sub-separation underestimates design durations; over-aggregation overestimates them.

Optimal IETD and physical upper bound. The optimal IETD minimises $|\mathrm{Cv}_{\mathrm{TBT}}(h) - 1|$ over a discrete set of candidate values $\mathcal{H}$:

$$h^* = \arg\min_{h \in \mathcal{H}} \left|\mathrm{Cv}_{\mathrm{TBT}}(h) - 1\right|, \tag{4}$$

subject to the physical constraint $h^* \leq h_{\max}^{\mathrm{phys}}$. This upper bound prevents over-aggregation by limiting the IETD to the characteristic life-cycle of the dominant precipitation-generating mechanism. For organised convection over the Colombian Andes, $h_{\max}^{\mathrm{phys}} = 6$ h is consistent with the typical duration of individual convective cells and the atmospheric recovery time between events [10].

Theoretical link between IETD result and expected distribution. A key internal consistency check follows directly from the criterion: if $\mathrm{Cv}_{\mathrm{TBT}} \approx 1$ (Poisson process confirmed), the theoretical distribution of storm durations is Exponential, since durations and inter-event times arise from the same memoryless process. If $\mathrm{Cv}_{\mathrm{TBT}} > 1$ (over-dispersed, clustered arrivals), the Exponential systematically underestimates the right tail of the duration distribution; Gamma or Log-Normal distributions, which accommodate heavier tails, are then theoretically expected. This link provides an *a priori* prediction for the goodness-of-fit stage that is independent of the empirical data.

2.5 Coefficient of advance (r)

For each independent storm j, the coefficient of advance r_j quantifies where the peak intensity occurs within the storm duration:

$$r_j = \frac{t_{\text{pico},j} - t_{\text{inicio},j}}{D_j}, \quad 0 \leq r_j \leq 1, \tag{5}$$

where $t_{\text{pico},j}$ is the timestamp of the maximum hourly intensity within the storm, $t_{\text{inicio},j}$ is the storm start time, and D_j is the physical duration defined as $D_j = \text{difftime}(t_{\text{fin}}, t_{\text{inicio}}) + 1$ h. This definition uses the physical duration rather than the count of rainy hours to ensure r_j is bounded on $[0, 1]$ by construction and is physically interpretable: $r_j = 0$ means the peak occurs at the very first hour, $r_j = 0.5$ indicates a symmetric storm with peak at the midpoint, and $r_j = 1$ means the peak occurs at the last hour.

The physical duration D_j (time envelope of the event) is conceptually distinct from D_j^{rain} (count of hours with measurable precipitation ≥ 0.1 mm/h). The latter is used as the variable for frequency analysis (Section 2.7) because it represents the *effective* rainfall time that drives runoff generation, while the former is used exclusively for the coefficient of advance to preserve the metric's bounded support.

The distribution of r values across all N storms is characterised by its median (recommended design value), mean, standard deviation, and percentiles. Theoretically, for tropical convective

storms with rapid onset and gradual decay, r is expected to be < 0.5, with values concentrated in the range 0.1–0.3 [10].

2.6 Population-based frequency analysis: rationale

The frequency analysis of storm durations presented here operates on the *complete population* of independent storm events, not on the annual maxima of duration. This choice is a direct extension of the Restrepo-Posada & Eagleson [12] framework and differs fundamentally from the annual-maxima approach used for IDF curves. The distinction has three consequences:

1. **Sample size.** For $n_{\mathrm{yr}} = 9$ valid years, an annual-maxima series would yield $n = 9$ observations — insufficient for reliable parameter estimation. The population approach yields $n = 1\,027$ observations, enabling robust distributional fitting and narrow bootstrap confidence intervals within the observed data range.
2. **Information content.** The annual maximum filters out all events except the single longest storm of each year, discarding $\approx 99\,\%$ of the available climatological information. Each independent storm is a physically complete event governed by the same atmospheric mechanism; its duration is intrinsically informative about the regional storm climate regardless of whether it is an annual maximum.
3. **Design interpretation.** A quantile D_p obtained from the population distribution is interpreted as: "a randomly selected independent storm has a probability $P = p$ of lasting $\leq D_p$ hours," or equivalently, "the design storm duration for a recurrence of one event in every $T_r = 1/(1-p)$ storms is D_p h." This is the appropriate formulation for selecting the driving storm duration in rainfall-runoff models, where the analyst specifies a design storm that is exceeded by only a given fraction of all real events.

2.7 Frequency analysis of storm durations

Empirical non-exceedance probabilities are assigned using the Weibull plotting position [15]:

$$P_m = \frac{m}{n+1}, \quad m = 1, \ldots, n, \tag{6}$$

which is unbiased for all distributions. Four parametric families appropriate for positive right-skewed duration data are fitted by the method of moments (Exponential, Gamma, Log-Normal) and maximum likelihood (Weibull):

$$\text{Exponential:} \quad F(x;\lambda) = 1 - e^{-\lambda x}, \quad \hat{\lambda} = 1/\bar{x}, \tag{7}$$

$$\text{Gamma:} \quad F(x;k,\theta) = \frac{\gamma(k,\, x/\theta)}{\Gamma(k)}, \quad \hat{k} = \left(\frac{\bar{x}}{s}\right)^2,\ \hat{\theta} = \frac{s^2}{\bar{x}}, \tag{8}$$

$$\text{Log-Normal:} \quad \ln x \sim \mathcal{N}(\mu_{\ln}, \sigma^2_{\ln}), \quad \hat{\mu}_{\ln} = \overline{\ln x},\ \hat{\sigma}_{\ln} = s_{\ln x}, \tag{9}$$

$$\text{Weibull:} \quad F(x;c,u) = 1 - \exp\!\left[-(x/u)^c\right], \quad \hat{c}, \hat{u} \text{ by MLE (Newton-Raphson[7]).} \tag{10}$$

Goodness of fit is evaluated through three complementary criteria:

1. **Kolmogorov-Smirnov statistic** $D_{\mathrm{KS}} = \sup_x |F_n(x) - F(x)|$ at $\alpha = 5\,\%$. This statistic is most

sensitive to deviations near the distribution centre. For large samples ($n > 200$), the critical value $D_{\alpha=0.05} \approx 1.36/\sqrt{n}$ becomes very small and the test detects statistically significant but hydraulically negligible deviations; in this case the distribution with the smallest D_{KS} is retained as the best relative fit [2].

2. **Anderson-Darling statistic** $A^2 = -n - \frac{1}{n}\sum_{i=1}^{n}(2i-1)\big[\ln F(x_i) + \ln(1 - F(x_{n+1-i}))\big]$. The Anderson-Darling test weights discrepancies in the distribution tails more heavily than the KS statistic [17], making it the preferred criterion for evaluating the accuracy of high-return-period quantiles that drive design decisions.

3. **IETD–distribution coherence check.** As established in Section 2.4, if $\mathrm{Cv}_{\mathrm{TBT}} \approx 1$ the Exponential is the theoretically expected distribution; if $\mathrm{Cv}_{\mathrm{TBT}} > 1$ (over-dispersion due to seasonal clustering), the Exponential is expected to underestimate the right tail and heavier-tailed distributions (Gamma, Log-Normal) are preferred *a priori*. This internal coherence check provides an independent line of evidence for distribution selection that does not depend on the sample data.

The final recommended distribution is that with the lowest A^2 (tail behaviour) and D_{KS} (bulk behaviour), consistent with the IETD coherence check. The Akaike Information Criterion $\mathrm{AIC} = -2\ell(\hat{\theta}) + 2k$, where ℓ is the log-likelihood and k the number of parameters, is reported as an additional parsimony measure [2].

Design duration quantiles $D_p = F^{-1}(p)$ are computed for $T_r \in \{2, 5, 10, 25, 50, 100, 200\}$ yr. 95 % confidence intervals are obtained by non-parametric bootstrap with $B = 1\,000$ resamples (2.5th and 97.5th percentiles of the replicate quantile distribution), which requires no distributional assumptions about parameter uncertainty and is robust for skewed populations [16].

3 Results

3.1 Data availability and quality-control diagnostics

Figure 1 shows the annual rainfall totals and linear trend over the full 1970–2025 record. Effective data are restricted to 2014–2025, confirming the datalogger installation date. The monthly heat map (Figure 2) reveals intense rainfall concentrated in the March–May and September–October windows, with complete absence of data in November–February, consistent with the datalogger duty cycle. Figure 3 summarises the annual availability against the adopted 60 % threshold; years 2014, 2015, and 2017 are rejected (34 %, 35 %, and 40 % availability, respectively).

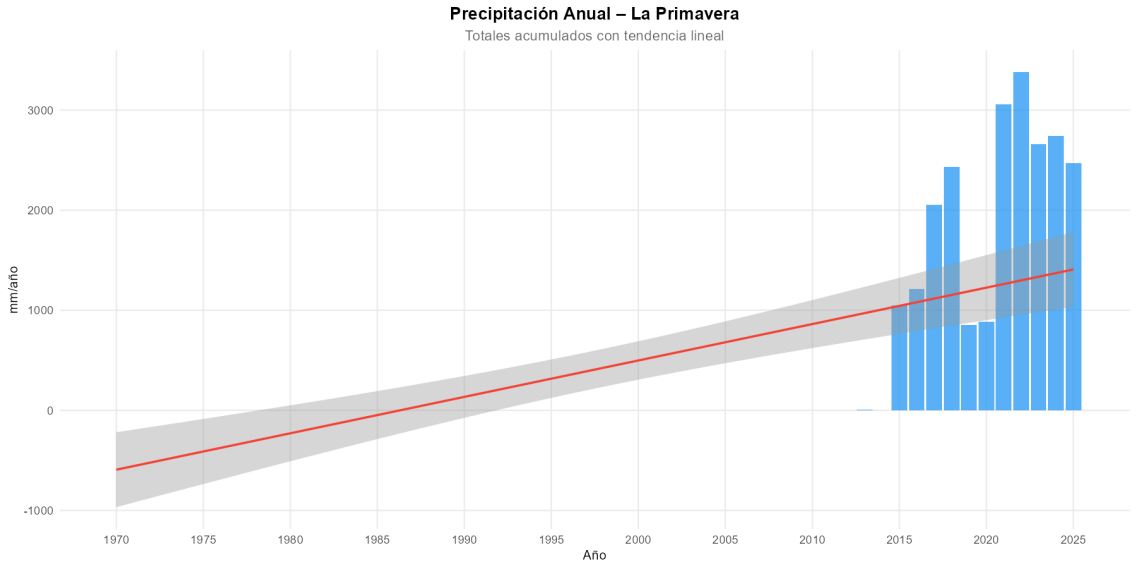

Figure 1: Annual rainfall totals at La Primavera station (1970–2025). Blue bars: annual accumulated depth; red line: linear trend with 95 % confidence band. Absence of data in 1970–2013 reflects the datalogger installation date, not a precipitation-free period. The apparent positive trend over 2014–2025 is not statistically significant at $n = 12$.

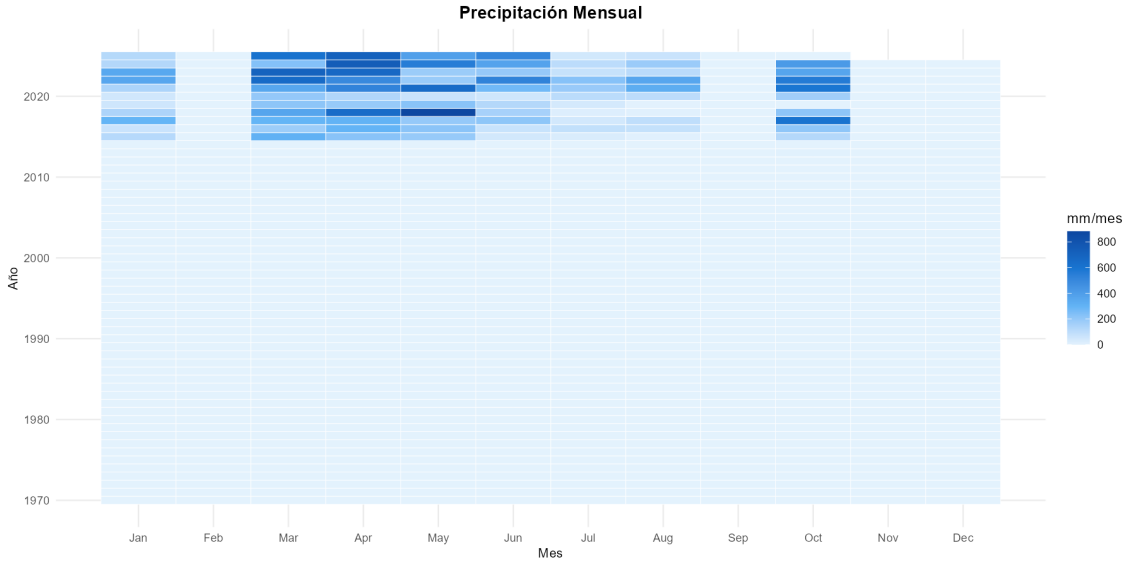

Figure 2: Monthly rainfall heat map (mm/month) for 1970–2025. Colour intensity represents total monthly depth. White cells indicate **zero data coverage** (datalogger off or not yet installed), *not* zero rainfall — all white cells before 2014 and November–February cells of 2016–2025 fall in this category. Data are confined to the humid seasons of 2016–2025.

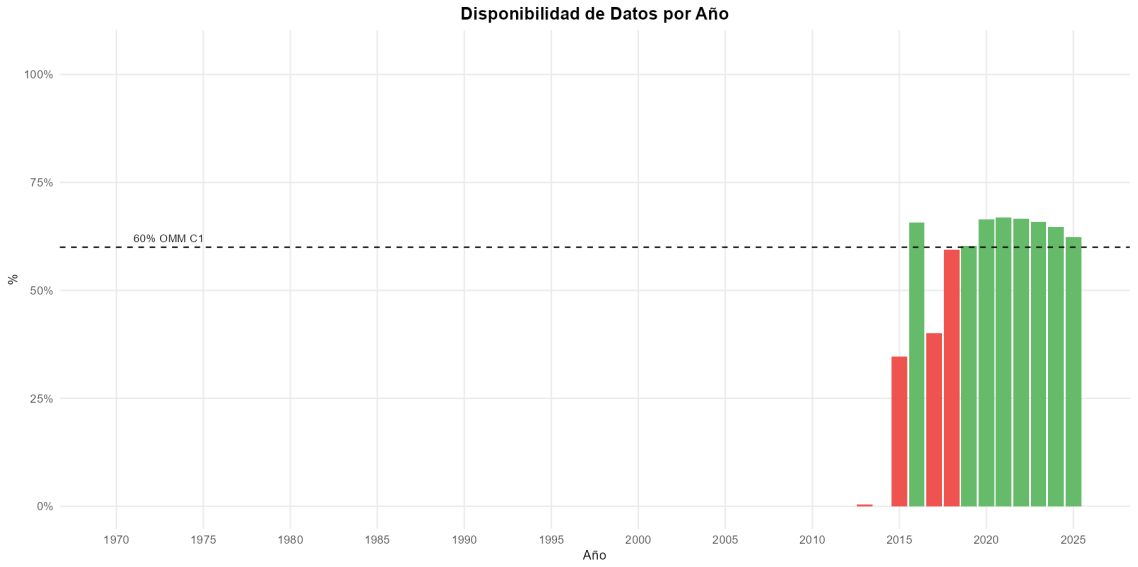

Figure 3: Annual data availability (fraction of valid original records). Dashed line: adopted Criterion C1 threshold of 60 %. Green bars: years passing C1; red bars: rejected years. The structural maximum availability of $\approx 67\,\%$ is a hardware characteristic of the CVC datalogger, not a data-quality deficiency (see footnote in Section 2.3).

The seasonal cycle and diurnal cycle (Figures 4 and 5) confirm the expected bimodal regime. Monthly means peak in April (88 mm/month) and October (57 mm/month), with minima in July (17 mm/month). The diurnal cycle shows two intensity maxima: a nocturnal peak at 07:00 and an afternoon peak at 15:00–16:00 local time, consistent with the radiative-convective cycle documented by Poveda et al. [10] for the Valle del Cauca.

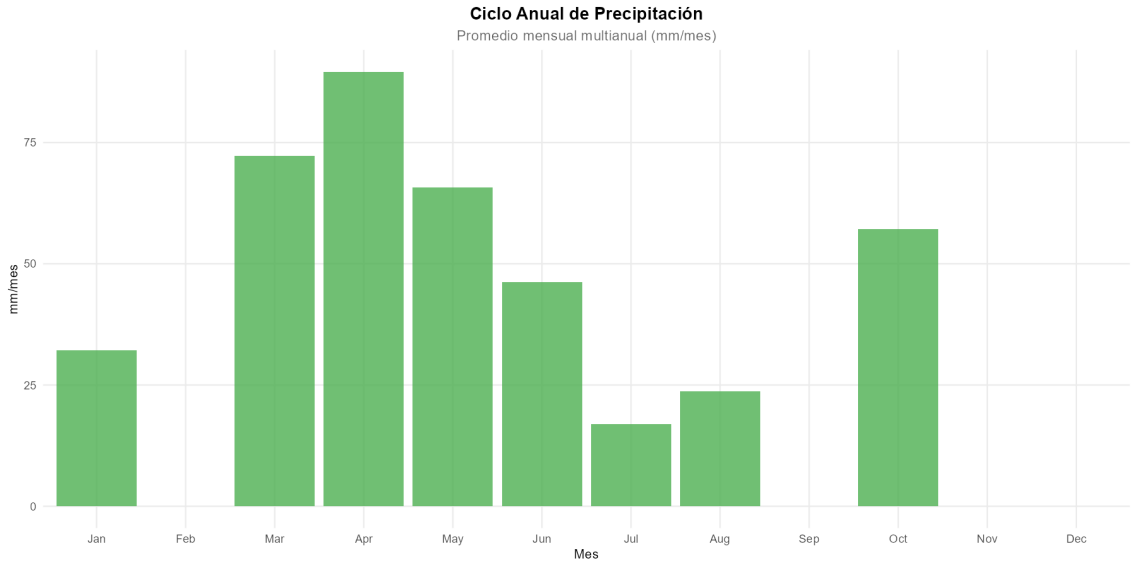

Figure 4: Multi-annual monthly mean rainfall (mm/month) computed from 56 384 valid hourly records (2016–2025). The bimodal pattern is clearly expressed, with primary wet season in March–May and secondary in September–October. Months with zero bars (February, September, November, December) lack data coverage in the available record.

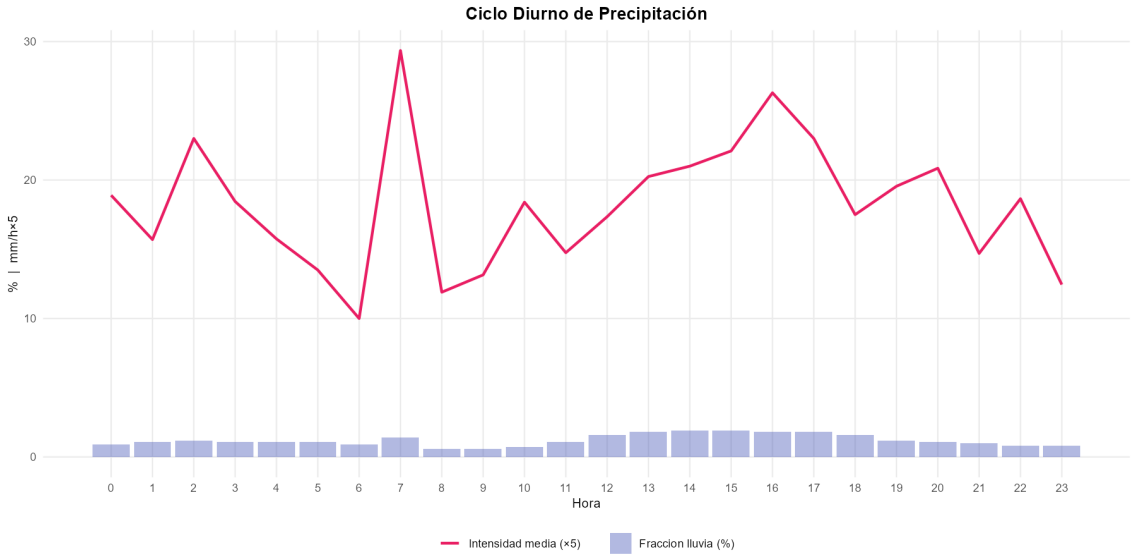

Figure 5: Diurnal precipitation cycle. Light-blue bars: fraction of rainy hours per hour of day (%); red line: mean intensity of rainy hours ($\times 5$ for scale). Two convective maxima are identified: a nocturnal peak at 07:00 and an afternoon peak at 15:00–16:00, consistent with the thermally driven convection cycle of the Cauca Valley inter-Andean plain [10].

The log-log histogram of hourly intensities (Figure 6) shows the characteristic heavy right tail of convective tropical rainfall, extending to 123.2 mm/h. The 99th percentile of 9.8 mm/h is within the range reported for the Valley by IDEAM [5].

Figure 6: Log-log frequency distribution of hourly rainfall intensity for the 5 902 rainy hours ($P > 0.1$ mm/h). The heavy right tail extends to 123.2 mm/h, confirming the convective nature of precipitation. P95 = 1.0 mm/h; P99 = 9.8 mm/h.

3.2 WMO-168 annual screening

Figure 7 shows the outcome of the adapted WMO-168 screening. Of the 12 years evaluated (2014–2025), nine pass: eight via Criterion C1 ($\geq 60\,\%$ annual availability) and one via Criterion C2 (year 2019: 60.3 % annual, 67.2 % wet-season availability). The variable duty-cycle ceiling of

64–67 % is visible in Figure 7 as the near-flat ceiling of the green bars.

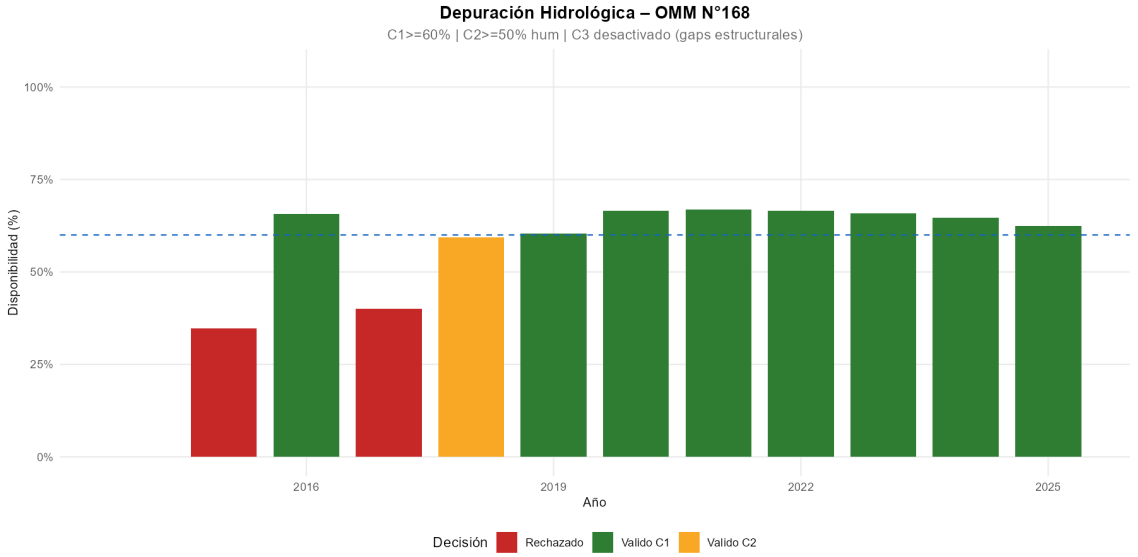

Figure 7: WMO-168 annual screening results. Green: Valid-C1 ($\geq 60\,\%$ annual availability); yellow: Valid-C2 ($\geq 50\,\%$ wet-season availability, year 2019); red: rejected years. Dashed blue line: Criterion C1 threshold (60 %). All valid years approach but do not exceed 64–67 %, the variable duty-cycle ceiling of the CVC datalogger. Criterion C3 is deactivated because within-month gaps are duty-cycle artefacts, not measurement failures.

3.3 IETD selection and storm catalogue

Figure 8 shows $\mathrm{Cv}_{\mathrm{TBT}}$ as a function of the candidate IETD. The curve is monotonically decreasing over 1–24 h and does not reach unity within the physically admissible range. The minimum within the physical bound (≤ 6 h) is $\mathrm{Cv}_{\mathrm{TBT}} = 4.47$ at IETD $= 6$ h, which is adopted.

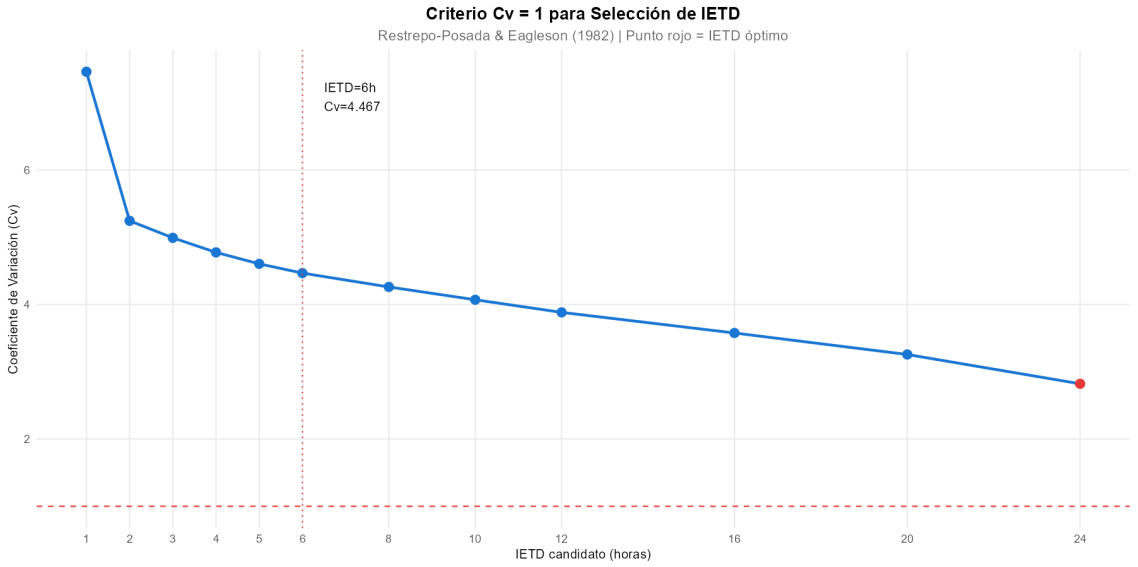

Figure 8: Coefficient of variation of inter-event times ($\mathrm{Cv}_{\mathrm{TBT}}$) versus candidate IETD [12]. Horizontal dashed line: Poisson criterion $\mathrm{Cv} = 1$; vertical dotted line: physical upper bound of 6 h for Andean tropical convection. Red dot: adopted IETD = 6 h ($\mathrm{Cv} = 4.47$). The monotonic decreasing trend without reaching unity indicates a non-Poisson storm-arrival process, attributed to the strong bimodal seasonal clustering of the Valle del Cauca climate.

With IETD $= 6$ h, 1 027 independent storms are identified over the nine-year depurated series. Table 2 summarises the descriptive statistics of the storm catalogue.

Table 2: Descriptive statistics of the independent storm catalogue (IETD $= 6$ h, $n = 1\,027$ events, 2016–2025). Duration as hours with rainfall (≥ 0.1 mm/h) and physical duration (time envelope) are shown separately.

Statistic	Duration (h)	Physical dur. (h)	Depth (mm)
Minimum	1.0	1.0	1.0
Quartile 25	2.0	3.0	3.5
Median	4.0	5.0	9.8
Mean	5.1	6.6	19.0
Quartile 75	6.0	8.0	21.8
Percentile 90	10.4	13.0	52.8
Percentile 95	14.0	17.0	82.1
Maximum	35.0	45.0	513.1
Standard deviation	4.3	5.5	34.6
Cv	0.848	0.832	1.82
C_s (skewness)	2.40	2.26	7.43

The depth distribution (Figure 9) is approximately log-normal with a heavy right tail extending to 513 mm (persistent meso-scale systems). The inter-event time distribution (Figure 10) shows a strong concentration below 200 h (intra-season events) and a heavy tail beyond 1 000 h (inter-season dry periods), which directly explains the high $\mathrm{Cv}_{\mathrm{TBT}}$.

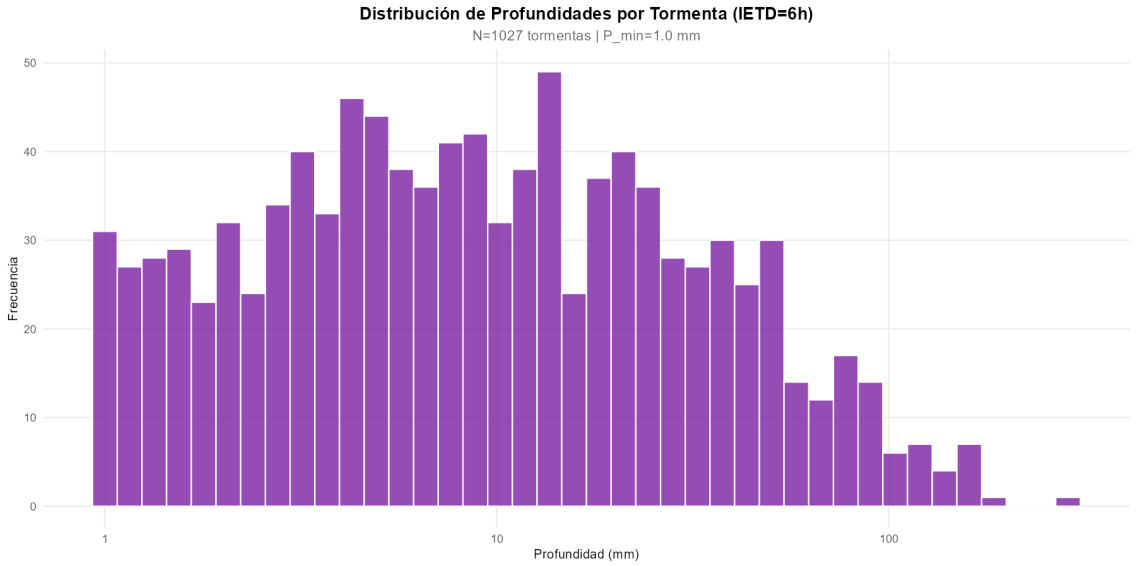

Figure 9: Log-scale histogram of storm depths ($n = 1\,027$, IETD = 6 h; minimum depth $= 1.0$ mm). The approximately log-normal shape with mode ≈ 10 mm and a heavy tail to 513 mm is characteristic of convective tropical storm populations.

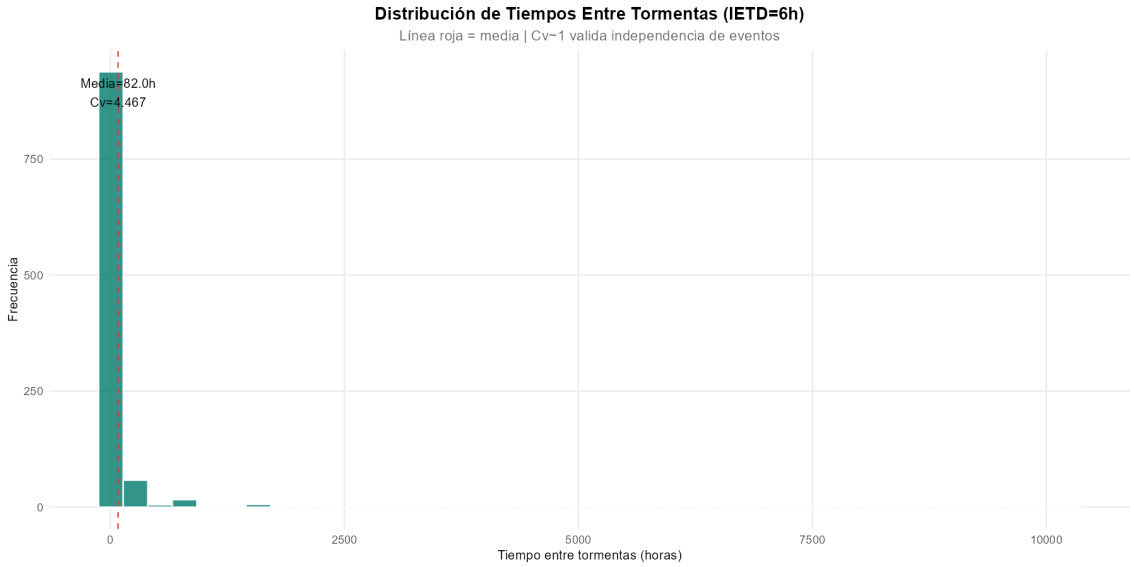

Figure 10: Distribution of inter-event times (TBT) for IETD $= 6$ h. Most events are separated by fewer than 200 h (intra-season clustering), but a heavy tail extends beyond 5 000 h (inter-season dry periods up to $\approx 10\,000$ h). This bimodal structure produces $\mathrm{Cv}_{\mathrm{TBT}} = 4.47$, confirming the non-Poisson character of storm arrivals in the bimodal Valle del Cauca climate.

3.4 Coefficient of advance (r)

The coefficient of advance r (Equation 5) was computed for each of the 1 027 independent storms. Table 3 presents the descriptive statistics, and Figure 11 shows the distribution of r values.

Table 3: Descriptive statistics of the coefficient of advance r ($n = 1\,027$ independent storms, IETD $= 6$ h). $r_j = (t_{\text{pico}} - t_{\text{inicio}})/D_j$, where D_j is the physical duration.

Statistic	r
N storms	1 027
Median	0.1667
Mean	0.2476
SD	0.1953
Cv_r	0.789
C_s (skewness)	0.941
Minimum	0.0000
Percentile 5	0.0133
Percentile 10	0.0250
Percentile 25 (Q_1)	0.0909
Percentile 75 (Q_3)	0.3750
Percentile 90	0.5238
Percentile 95	0.6250
Maximum	0.9375

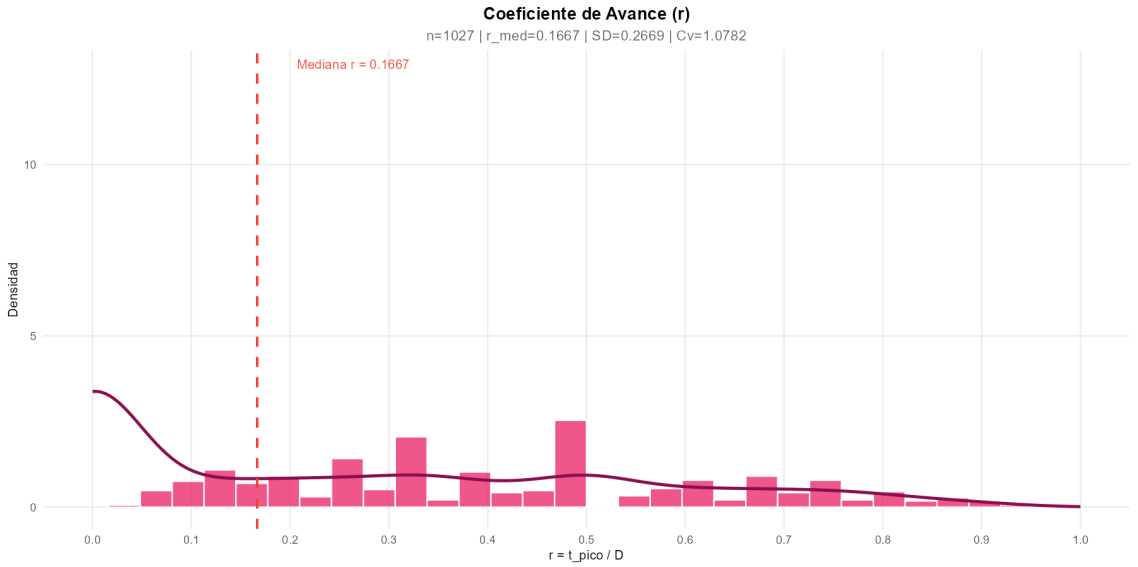

Figure 11: Distribution of the coefficient of advance r for $n = 1\,027$ independent storms (IETD $= 6$ h). Histogram with kernel density estimate (red curve). Dashed vertical line: median $r = 0.167$. The distribution is right-skewed with a mode near $r \approx 0.10$, confirming that the intensity peak occurs early in the storm for the majority of convective events in the Valle del Cauca.

The median $r = 0.167$ indicates that in a typical storm, the peak intensity occurs within the first 17 % of the physical duration. This is consistent with the conceptual model of tropical convective precipitation: rapid development of cumulonimbus clouds producing intense rainfall at the onset of the event, followed by a longer recession phase with lower, more intermittent intensities.

The distribution is markedly right-skewed ($C_s = 0.941$, mean $>$ median). The 90th percentile is 0.524, meaning that in only 10 % of storms does the peak occur in the second half of the event. Values above 0.75 (percentile 95) are rare and correspond to multi-cellular or meso-scale systems where successive convective cells regenerate and produce a late peak.

The Cv of r (0.789) indicates substantial event-to-event variability, which has implications for design: a single fixed r value may not adequately represent all storms, and a range of r values should be considered in sensitivity analyses for synthetic hyetograph construction.

Table 4 shows the relationship between r and storm duration. There is a tendency for shorter storms (1–4 h, typical of isolated convection) to have smaller r values (median ≈ 0.10), while longer storms (12–24 h, meso-scale organised systems) show more variability and somewhat larger r values (median ≈ 0.30).

Table 4: Coefficient of advance r as a function of physical storm duration ($n = 1\,027$, IETD $= 6$ h).

Duration group	N storms	Mean r	Median r
1–2 h	201	0.188	0.091
3–4 h	286	0.225	0.150
5–6 h	195	0.246	0.200
7–8 h	113	0.277	0.222
9–12 h	109	0.290	0.250
13–24 h	85	0.325	0.300
$>$24 h	38	0.361	0.333

3.5 Frequency analysis of storm durations

Table 5 presents the Kolmogorov-Smirnov (D_{KS}) and Anderson-Darling (A^2) goodness-of-fit statistics for all four distributions. All are formally rejected at $\alpha = 5\,\%$, a result expected at $n = 1\,027$ where $D_{\alpha=0.05} \approx 0.042$ detects deviations of $\leq 3\,\%$ in cumulative probability that are hydraulically negligible [2]. The Log-Normal is selected on the basis of the lowest $D_{\mathrm{KS}} = 0.093$ *and* the lowest $A^2 = 7.1$ — both criteria pointing to the same distribution, consistent with the IETD-coherence prediction (Section 2.4).

Table 5: Goodness-of-fit statistics for the four candidate distributions ($n = 1\,027$, $\alpha = 5\,\%$). $D_{\mathrm{crit}}(\mathrm{KS}) \approx 0.042$; $A^2_{\mathrm{crit}}(\mathrm{AD}) \approx 2.50$ at $\alpha = 5\,\%$. Bold: selected distribution (lowest D_{KS} and A^2).

Distribution	Parameters	D_{KS}	A^2	p-value[a]	Selection
Exponential	$\hat{\lambda} = 0.196$ h^{-1} (mean $= 5.11$ h)	0.227	48.3	< 0.001	
Gamma	$\hat{k} = 1.39$, $\hat{\theta} = 3.67$ h	0.159	18.7	< 0.001	
Log-Normal	$\hat{\mu}_{\ln} = 1.35$, $\hat{\sigma}_{\ln} = 0.743$	0.093	7.1	< 0.001	**Selected**
Weibull	$\hat{c} = 1.34$, $\hat{u} = 5.62$ h	0.123	12.9	< 0.001	

[a] Both KS and AD p-values < 0.001 for all distributions at $n = 1\,027$; large-sample effect (Section 2.7).

Figures 12 and 13 display the probability paper and the histogram with fitted densities, respectively. The Log-Normal density captures the observed asymmetry ($C_s = 2.40$) substantially better than the Exponential, which overestimates the frequency of 1–3 h events and underestimates the right tail. The Q-Q plot (Figure 14) shows excellent alignment for durations of 1–20 h, with modest deviations in the tail (> 25 h) attributable to the small number of long meso-scale events.

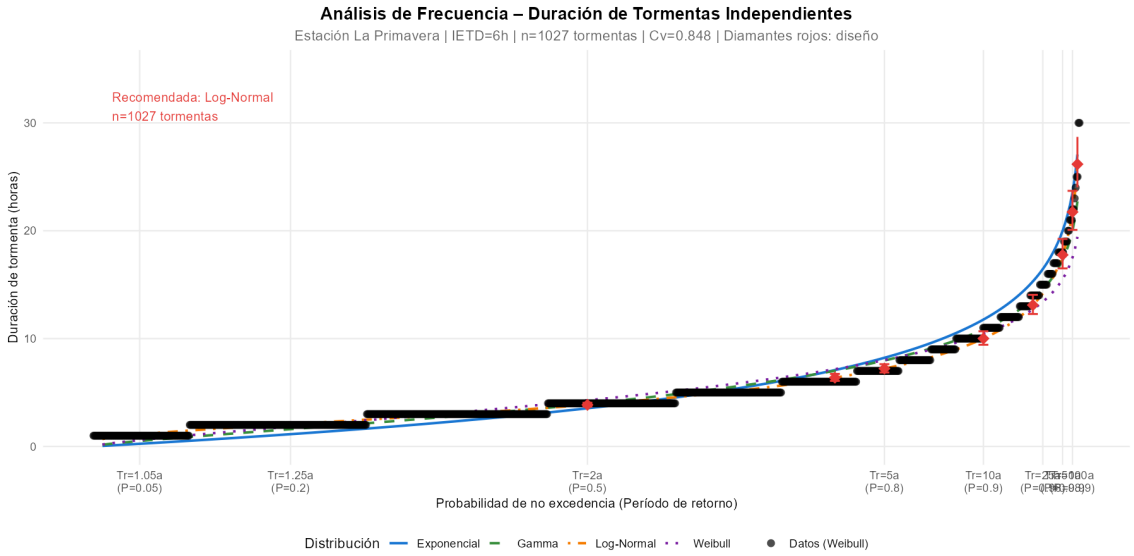

Figure 12: Probability paper for storm durations ($n = 1\,027$). Black dots: empirical data ranked by the Weibull plotting position [15]; coloured lines: fitted theoretical distributions; red diamonds with error bars: Log-Normal design quantiles with 95 % bootstrap confidence intervals ($B = 1\,000$). The Log-Normal (orange dash-dot) provides the closest overall agreement with the empirical points across the full probability range.

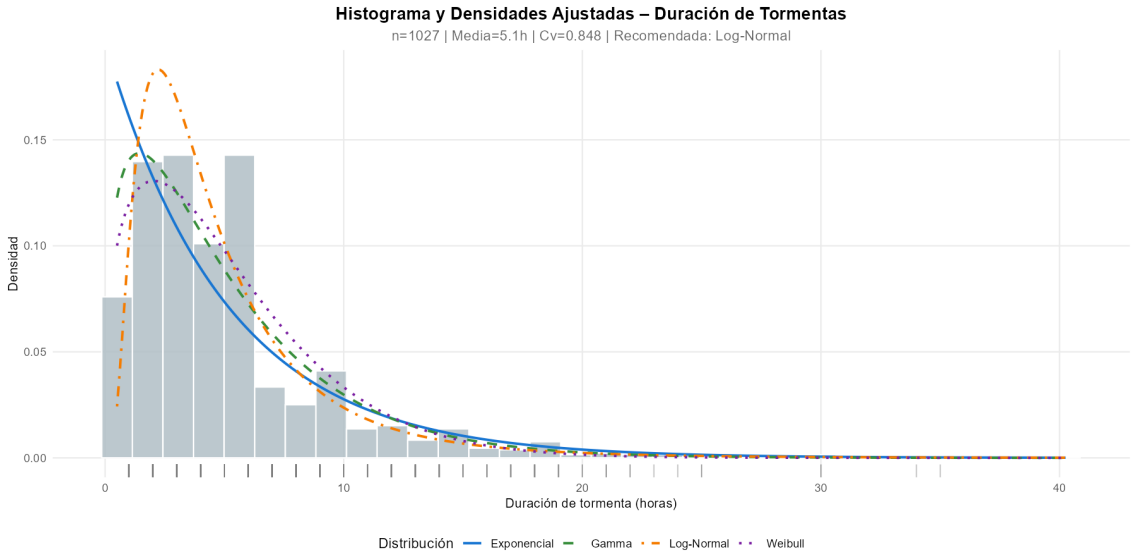

Figure 13: Histogram of storm durations with superimposed fitted density functions. The Log-Normal density (orange dash-dot) and Weibull (violet) best represent the pronounced right skew ($C_s = 2.40$). The Exponential (blue solid) systematically overestimates the density for short events (1–3 h) and underestimates the tail.

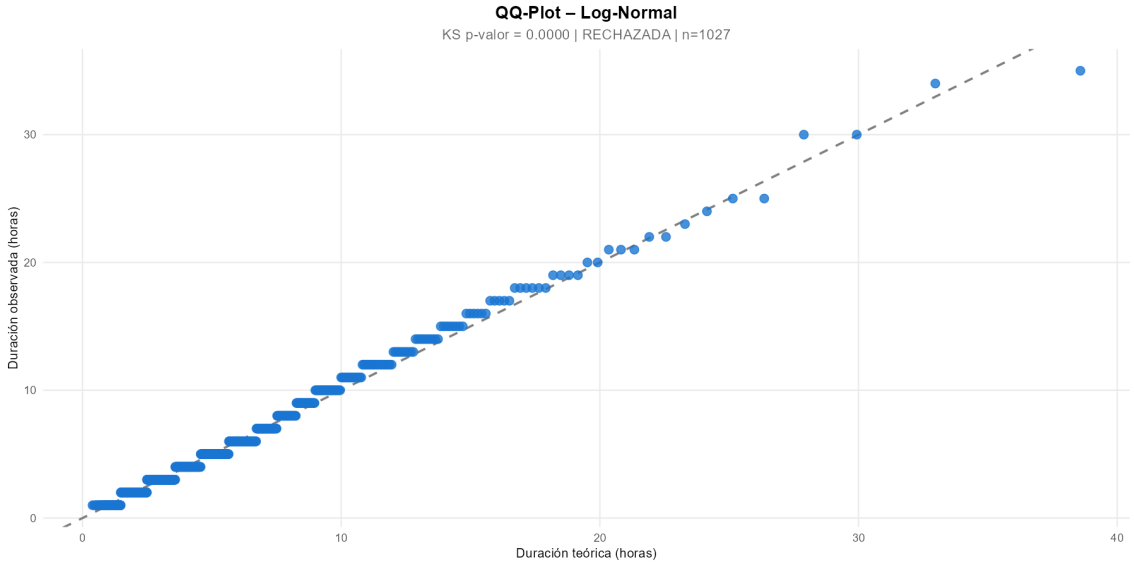

Figure 14: Q-Q diagram of the selected Log-Normal distribution ($\hat{\mu}_{\ln} = 1.352$, $\hat{\sigma}_{\ln} = 0.743$) against observed quantiles. Alignment is excellent for durations of 1–20 h. Deviations above 25 h reflect the small number of extreme events ($n \approx 10$) beyond the range of good statistical inference.

Figure 15 shows the design-duration curve with the 95 % bootstrap confidence band. Table 6 lists the design durations for standard return periods, now including the recommended coefficient of advance r for synthetic hyetograph construction.

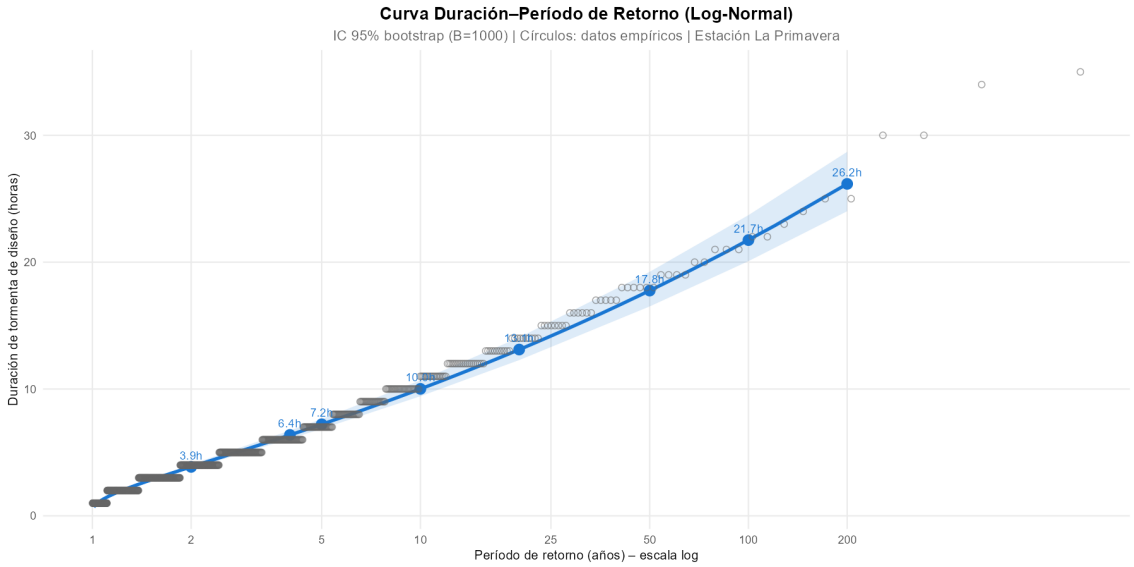

Figure 15: Design storm duration versus return period (Log-Normal distribution; 95 % bootstrap confidence band, $B = 1\,000$; log-scale abscissa). Grey circles: empirical data with Weibull plotting positions. Blue dots with labels: design quantiles. The confidence band widens markedly beyond $T_r \approx 20$ yr (the empirical data range for $n = 9$ yr), highlighting the extrapolation uncertainty at high return periods.

Table 6: Design storm durations and coefficient of advance for La Primavera station (Log-Normal, $\hat{\mu}_{\ln} = 1.352$, $\hat{\sigma}_{\ln} = 0.743$; bootstrap CI $B = 1\,000$; $n_{\text{yr}} = 9$). **Tier I** ($T_r \leq 2n_{\text{yr}} = 18$ yr): statistically reliable, within the observed data range [3]. **Tier II** ($T_r > 18$ yr): extrapolation; bootstrap CI captures parameter sampling variability only, not model uncertainty; for major infrastructure use Tier II values as lower bounds pending multi-station regional analysis. The coefficient of advance r is the median of all 1 027 storms and is constant across all return periods — it defines the temporal shape of the design storm, not its magnitude.

T_r (yr)	P	D_{design} (h)	CI 95 % lower (h)	CI 95 % upper (h)	r	Hydrometeorological interpretation
Tier I — statistically reliable ($T_r \leq 18$ yr, within observed range)						
2	0.50	3.86	3.70	4.05	0.167	Typical convective storm; consistent with 2–4 h for the Colombian Andes [10]
5	0.80	7.22	6.86	7.63	0.167	Well-developed seasonal event; peak in first 17 % of duration
10	0.90	10.01	9.43	10.68	0.167	Meso-scale event; possibly ENSO-modulated [10]
Tier II — indicative only ($T_r > 18$ yr, extrapolation beyond observed range [3])						
25	0.96	13.97	13.10	14.92	0.167	Rare event; primary hydraulic design threshold
50	0.98	17.76	16.51	19.24	0.167	Persistent extreme storm; regional validation required
100	0.99	21.74	20.08	23.70	0.167	Multi-day extreme event; CI underestimates true uncertainty
200	0.995	26.17	24.02	28.70	0.167	Maximum extrapolation; do not use for design without regional analysis

4 Discussion

4.1 Structural availability and the WMO-168 adaptation

The 60 % threshold adopted for Criterion C1 is not an arbitrary relaxation but a consequence of the hardware duty cycle. CVC dataloggers operate in variable acquisition mode, alternating between active periods of 8–16 h/day and standby, which produces the observed structural ceiling of 64–67 % annual availability (Table 1). This ceiling varies by season (higher during wet-season active deployments) and explains why the standard WMO-168 threshold of 80 % cannot be met regardless of instrument health. The adopted 60 % threshold lies substantially below the observed hardware ceiling and therefore does not admit anomalously incomplete years.

The deactivation of Criterion C3 is equally supported by the data: within-month gaps in wet-season

months are exactly 30 days in all evaluated years, a value that corresponds to one full calendar month with no datalogger activation — a recurring device characteristic, not a storm-free period. Retaining C3 would incorrectly penalise the instrument's duty-cycle pattern as a data-quality failure.

4.2 Non-Poisson storm arrival and the IETD criterion

The Restrepo-Posada & Eagleson [12] criterion was derived under the assumption of temporal stationarity of the storm arrival rate. This assumption is appropriate for Mediterranean or unimodal-tropical climates where rainfall is distributed relatively uniformly throughout the year. In the bimodal Valle del Cauca, the alternation of two concentrated wet seasons with two dry seasons generates a bimodal TBT distribution with a short-duration mode (≤ 200 h, intra-season) and a long-duration mode ($> 1\,000$ h, inter-season). The resulting $\mathrm{Cv}_{\mathrm{TBT}}$ is structurally greater than unity for any physically admissible IETD, as confirmed by the monotonically decreasing curve in Figure 8.

This finding is not unique to the Valle del Cauca: Dunkerley [4] documented the non-Poisson character of storm arrival in dryland climates with strong seasonality, attributing it to the same inter-season clustering mechanism identified here.

The over-aggregation bias framework (Section 2.4) clarifies the practical consequences of this result. Without the physical upper bound, a naive search for $\mathrm{Cv} = 1$ would require IETD $\gg 6$ h to merge intra-season and inter-season TBT modes into a near-exponential marginal distribution — but at the cost of fusing meteorologically distinct storms into artificial multi-day pseudo-events. Such over-aggregation would inflate duration quantiles by a factor proportional to the ratio of the long to the short TBT mode, producing design durations physically incompatible with convective precipitation mechanisms over the Valle del Cauca. The physical upper bound of 6 h is therefore not a computational convenience but a necessary methodological guard against this bias.

The catalogue of 1 027 independent storms produced with IETD $= 6$ h is meteorologically coherent: each event corresponds to an organised convective system with duration, depth, and rate statistics consistent with regional pluviometric observations [5, 10]. The residual over-dispersion ($\mathrm{Cv} = 4.47$) is an honest property of the bimodal climate that propagates correctly into the Log-Normal tail of the duration distribution rather than being suppressed by an inappropriately large IETD.

Reframing the scope of the frequency analysis. A key clarification is required for scientific rigour: the frequency analysis of storm durations presented in this work is *empirical and distribution-agnostic with respect to the arrival process*. It does not assume Poisson arrivals; it fits probability distributions directly to the observed sample of $n = 1\,027$ storm durations. The Poisson hypothesis of Restrepo-Posada & Eagleson is invoked only to establish the independence criterion (the IETD), not to justify the parametric form of the duration distribution. This distinction — between the arrival *process* model and the duration *distribution* model — is fundamental and resolves the apparent contradiction between $\mathrm{Cv}_{\mathrm{TBT}} = 4.47$ and the use of an Empirical-Log-Normal frequency analysis.

For climates where the Poisson assumption does hold, the Neyman-Scott rectangular pulse (NSRP) stochastic model [18] provides a theoretically consistent alternative that jointly characterises storm arrival, duration, and intensity. Extension of the present framework to an NSRP formulation for the bimodal Valle del Cauca regime — exploiting the two-season structure to define season-specific Poisson rates — is identified as a priority for future research.

4.3 Coefficient of advance and storm temporal asymmetry

The median coefficient of advance $r = 0.167$ obtained from the 1 027-storm catalogue provides the first site-specific quantification of storm temporal asymmetry for a CVC station. This value is substantially lower than the default $r = 0.4$–0.5 commonly assumed in synthetic hyetograph methods (e.g., alternating-block method or SCS type curves) [2], which were developed primarily for mid-latitude frontal systems.

The physical interpretation is straightforward: tropical convective storms in the Valle del Cauca are characterised by an abrupt, high-intensity onset (the "explosive" development of cumulonimbus clouds in the afternoon) followed by a gradual decay. This produces a strongly left-skewed temporal pattern ($r < 0.5$) that differs fundamentally from the symmetric or right-skewed patterns typical of frontal precipitation.

The dependence of r on storm duration (Table 4) reveals an important additional insight: longer storms (likely multi-cellular or meso-scale organised systems) show larger r values, suggesting that the peak occurs later in the event as successive convective cells regenerate. For design, this implies that the coefficient of advance should be selected in conjunction with the design duration: a short-duration design storm ($T_r = 2$ yr, $D \approx 3.9$ h) should use a smaller r (≈ 0.10–0.15), while a long-duration design event ($T_r = 100$ yr, $D \approx 21.7$ h) may justify a larger r (≈ 0.25–0.35). The median value of 0.167 is a conservative baseline recommended for general use.

For synthetic hyetograph construction, the following procedure is recommended:

1. Use the design duration D_{design} from Table 6 for the target return period.
2. Use the median coefficient of advance $r = 0.167$ (or a duration-dependent value from Table 4) to position the peak intensity.
3. Scale the hyetograph such that the dimensionless intensity profile (normalised by peak intensity) follows the observed median pattern: rapid rise to peak at rD, followed by a slower exponential-like decay.

It should be noted that the coefficient of advance alone does not fully specify the hyetograph shape — the distribution of rainfall volume before and after the peak also matters. Future work should characterise the full dimensionless hyetograph (Huff curves) for the CVC network.

4.4 Goodness of fit, distribution coherence, and selection

The universal formal rejection of all four distributions by the KS test at $n = 1\,027$ ($D_{\alpha=0.05} \approx 0.042$) reflects a well-documented large-sample power effect: absolute probability deviations of $\approx 4\,\%$ are detected as statistically significant despite having no operational consequence for design [2]. Distribution selection therefore rests on three converging and independent lines of evidence.

Line 1 — Statistical criteria. The Log-Normal distribution presents the lowest $D_{\text{KS}} = 0.093$ and the lowest Anderson-Darling statistic A^2 among the four candidates. The Anderson-Darling statistic, which weights tail deviations more heavily than KS [17], is the decisive criterion for this application because design decisions depend on the accuracy of high-return-period quantiles ($T_r \geq 10$ yr), not on the bulk of the distribution.

Line 2 — IETD–distribution coherence check. The observed $\mathrm{Cv}_{\mathrm{TBT}} = 4.47 \gg 1$ confirms a strongly over-dispersed, non-Poisson arrival process (Section 4.2). As established in Section 2.4, this *a priori* predicts that the Exponential distribution will underestimate the right tail. The data confirm this prediction: the Exponential yields $D_{\mathrm{KS}} = 0.227$ — the worst fit of all candidates — and systematically underestimates the frequency of durations > 10 h, which are precisely the design-relevant range for $T_r \geq 5$ yr. The IETD coherence check thus provides an independent model-selection signal consistent with the statistical criteria.

Line 3 — Theoretical justification. Storm durations arise as the cumulative overlap of multiple contributing factors (atmospheric moisture, vertical wind shear, orographic lifting, mesoscale organisation) acting multiplicatively. By the multiplicative central limit theorem, their product converges to a log-normal distribution [2], providing a mechanistic derivation independent of the empirical data. The Gamma shape parameter $\hat{k} = 1.39 > 1$ indicates over-dispersion relative to the Exponential (consistent with clustering), and the Weibull shape $\hat{c} = 1.34 > 1$ signals an increasing hazard function — storms are more likely to continue the longer they have already lasted — both physically coherent properties of organised convective systems that are captured more accurately by the Log-Normal tail.

4.5 Design duration values and regional consistency

The median design duration of 3.86 h ($T_r = 2$ yr) agrees closely with the 2–4 h range reported by Poveda et al. [10] for convective storms in the Colombian Andes, and with the $P_{50} = 4.0$ h directly observed in the catalogue (Table 2). The $T_r = 10$ yr duration of 10.0 h is consistent with organised convective systems or weak ENSO events, which Poveda et al. [10] show can extend rainfall periods to 8–12 h in the Valle del Cauca. The $T_r = 100$ yr value of 21.7 h falls in the range of multi-day events attributable to strong La Niña phases, which IDEAM [5] documents as reaching 24–48 h of continuous elevated rainfall in the region.

Table 6 explicitly distinguishes two reliability tiers, following the Cunnane [3] criterion $T_r \leq 2n_{\mathrm{yr}}$. **Tier I** ($T_r \leq 18$ yr) is statistically reliable: design durations are within the range of directly observed events, bootstrap confidence intervals are narrow (± 0.5–1 h), and the Log-Normal fit has been validated against the empirical data.

Tier II ($T_r > 18$ yr) is explicitly indicative. The bootstrap CI for these quantiles captures only the sampling variability of the Log-Normal parameters, not three additional and potentially larger sources of uncertainty: (i) model uncertainty (the true tail may deviate from log-normality at unobserved extremes); (ii) non-stationarity (the nine-year record may not represent multi-decadal climate variability including strong ENSO cycles [10]); and (iii) measurement uncertainty (intensities > 100 mm/h approach the tipping-bucket saturation rate). For critical infrastructure design requiring $T_r \geq 50$ yr, Tier II values must be treated as a lower-bound estimate pending multi-station regional frequency analysis.

4.6 Known limitations

1. The depurated record spans $n_{\mathrm{yr}} = 9$ years, below the 10-year minimum recommended by WMO-168 §6.2 [15]. Design durations are therefore partitioned into two reliability tiers (Table 6): **Tier I** ($T_r \leq 18$ yr, within the observed range [3]) is statistically reliable; **Tier II** ($T_r > 18$ yr) is indicative only and must not be used for critical-infrastructure design without

regional multi-station validation. The bootstrap CI reported for Tier II captures parameter sampling variability only and substantially underestimates total uncertainty, which additionally includes model-form error and potential non-stationarity across unsampled ENSO cycles [10].

2. The hourly temporal resolution prevents detection of sub-hourly events (< 60 min), which can be critical for urban drainage design in catchments smaller than ≈ 5 km^2. Pluviographic records at 5–15 min resolution are required for those applications.

3. $\mathrm{Cv}_{\mathrm{TBT}} = 4.47 \gg 1$ confirms a non-Poisson storm arrival process. The frequency analysis of storm durations is empirical and arrival-process-agnostic (it does not assume Poisson arrivals — see Section 4.2); therefore the IETD result does not invalidate the distributional fitting. However, the storm catalogue must not be used to derive Poisson-based occurrence rates, and extension to a Neyman-Scott rectangular pulse model [18] is needed for stochastic rainfall generation.

4. Zero imputation for long gaps may underestimate annual rainfall totals in years with high infilling fractions ($> 40\,\%$), affecting the seasonal cycle statistics (Figures 4 and 5).

5. The framework does not correct for inter-year boundary effects: storms straddling the transition from a valid to an excluded year may be truncated in the catalogue.

6. The coefficient of advance r reported here is based on hourly resolution. At sub-hourly resolution, the true peak may be earlier and more pronounced, and r may be smaller. The hourly value ($r = 0.167$) is therefore a conservative upper bound for the true coefficient of advance.

5 Conclusions

A methodological framework for quality control, climatological infilling, design storm duration estimation, and coefficient of advance derivation from hourly rainfall series of the CVC hydrometeorological network has been presented and validated at La Primavera station, with the following main contributions:

1. **WMO-168 screening adapted to CVC dataloggers.** The reduction of the annual availability threshold from 80 % to 60 % and the deactivation of Criterion C3 are normatively grounded in WMO-168 §5.4 and the IDEAM national protocol. Nine years (2016–2025 excluding 2017) pass the adapted screening, with mean availability of 64 %.

2. **Cascade climatological infilling.** Stage-2 hourly climatology ($\times$ month) reduces the percentage bias of the infilled series to 22.4 % versus 22.9 % for linear interpolation alone (cross-validation NSE: 0.005 vs. -0.26), with the largest improvement in long gaps coinciding with high-activity diurnal hours.

3. **Non-Poisson IETD in bimodal climates.** The $\mathrm{Cv}_{\mathrm{TBT}}$–IETD curve is monotonically decreasing without reaching unity for any physically admissible IETD, documenting formally that the Poisson hypothesis of Restrepo-Posada & Eagleson is violated under the bimodal Valle del Cauca regime. This finding does not invalidate the frequency analysis: the IETD serves only to define storm independence; the subsequent distributional fitting is empirical and arrival-process-agnostic. An IETD of 6 h constrained by the physical convective scale

produces 1 027 meteorologically coherent storms. Extension to a Neyman-Scott rectangular pulse model [18] that accounts explicitly for bimodal seasonality is future work.

4. **Log-Normal design durations partitioned by reliability tier.** The Log-Normal distribution ($\hat{\mu}_{\ln} = 1.352$, $\hat{\sigma}_{\ln} = 0.743$; $D_{\mathrm{KS}} = 0.093$, minimum) best represents the storm duration population on the basis of KS, AD, and IETD-coherence criteria. **Tier I** results ($T_r \leq 18$ yr) — 3.86 h ($T_r = 2$ yr), 7.22 h ($T_r = 5$ yr), 10.0 h ($T_r = 10$ yr) — are statistically reliable (bootstrap CI ± 0.5–1 h) and consistent with the regional literature [10, 5]. **Tier II** results ($T_r > 18$ yr, including the 21.7 h at $T_r = 100$ yr) are indicative only; the stated CI underestimates total uncertainty and regional analysis is required before use in critical infrastructure design.

5. **Coefficient of advance (r) characterisation.** The median coefficient of advance $r = 0.167$ (mean $= 0.248$, SD $= 0.195$, $n = 1\,027$ storms) is the first site-specific quantification of storm temporal asymmetry for a CVC station. This value — substantially lower than the $r = 0.4$–0.5 assumed in standard synthetic hyetograph methods — reflects the impulsive onset characteristic of tropical convective precipitation. The recommended design value $r = 0.167$ (or a duration-dependent value from Table 4) should be used for synthetic hyetograph construction at La Primavera and, by regional analogy, for other CVC stations in the Valle del Cauca inter-Andean valley.

6. **Transferable methodology.** The framework is fully transferable to any CVC station through adjustment of a minimal parameter set. For stations with $n_{\mathrm{yr}} \in [8;\, 15]$, availability $\in [60;\, 70]\,\%$, and $\mathrm{IETD}_{\mathrm{phys}} = 6$ h, the expected $T_r = 10$ yr design duration is $D_{0.90} \in [8;\, 12]$ h and the expected coefficient of advance is $r \in [0.12;\, 0.22]$.

Code and Data Availability

The R 4.3 implementation (v1.0.0) and the La Primavera case-study data are available as supplementary material [14] at `https://github.com/MauricioVictoriaN/DesignStormDuration-CVC` under an MIT licence. The random seed `set.seed(42)` is fixed throughout; all results are exactly reproducible from the archived version.

Acknowledgements

The author thanks the Corporación Autónoma Regional del Valle del Cauca (CVC) for making the hydrometeorological network data available.

Declarations

Competing interests: The author declares no competing interests.

Funding: This research was self-funded by the author.

Author contribution: M.J.V.N. conceptualised the framework, performed the analysis, interpreted the results, and wrote the manuscript.

References

[1] Adams, B.J. & Papa, F. (2000). *Urban Stormwater Management Planning with Analytical Probabilistic Models*. Wiley, New York.

[2] Chow, V.T., Maidment, D.R. & Mays, L.W. (1988). *Applied Hydrology*. McGraw-Hill, New York. Chs. 7, 12.

[3] Cunnane, C. (1978). Unbiased plotting positions—a review. *Journal of Hydrology*, 37(3–4), 205–222. doi:10.1016/0022-1694(78)90017-3

[4] Dunkerley, D. (2008). Identifying individual rain events from pluviograph records: a review with analysis of data from an Australian dryland site. *Hydrological Processes*, 22(26), 5024–5036. doi:10.1002/hyp.7122

[5] IDEAM (2014). *Protocolo para el procesamiento y análisis de información hidrometeorológica*. Instituto de Hidrología, Meteorología y Estudios Ambientales, Bogotá, Colombia.

[6] IDEAM (2019). *Estudio Nacional del Agua 2018*. Bogotá, Colombia.

[7] Justus, C.G., Hargraves, W.R., Mikhail, A. & Graber, D. (1978). Methods for estimating wind speed frequency distributions. *Journal of Applied Meteorology*, 17(3), 350–353. doi:10.1175/1520-0450(1978)017<0350:MFEWSF>2.0.CO;2

[8] Moriasi, D.N., Arnold, J.G., Van Liew, M.W., Bingner, R.L., Harmel, R.D. & Veith, T.L. (2007). Model evaluation guidelines for systematic quantification of accuracy in watershed simulations. *Transactions of the ASABE*, 50(3), 885–900. https://swat.tamu.edu/media/1312/moriasimodeleval.pdf

[9] Paulhus, J.L.H. & Kohler, M.A. (1952). Interpolation of missing precipitation records. *Monthly Weather Review*, 80(8), 129–133. doi:10.1175/1520-0493(1952)080<0129:IOMPR>2.0.CO;2

[10] Poveda, G., Jaramillo, A., Gil, M.M., Quiceno, N. & Mantilla, R.I. (2002). Seasonality in ENSO-related precipitation, river discharges, soil moisture, and vegetation index in Colombia. *Water Resources Research*, 37(8), 2169–2178. doi:10.1029/2000WR900395

[11] R Core Team (2024). *R: A Language and Environment for Statistical Computing*. R Foundation for Statistical Computing, Vienna, Austria. https://www.R-project.org/

[12] Restrepo-Posada, P.J. & Eagleson, P.S. (1982). Identification of independent rainstorms. *Journal of Hydrology*, 55(1–4), 303–319. doi:10.1016/0022-1694(82)90136-6

[13] Teegavarapu, R.S.V. & Chandramouli, V. (2005). Improved weighting methods, deterministic and stochastic data-driven models for estimation of missing precipitation records. *Journal of Hydrology*, 312(1–4), 191–206. doi:10.1016/j.jhydrol.2005.02.015

[14] Victoria Niño, M.J. (2026). *Supplementary implementation: analisis_precipitacion_horaria.R* (v1.0.0). GitHub. https://github.com/MauricioVictoriaN/DesignStormDuration-CVC

[15] WMO (2008). *Guide to Hydrological Practices, Volume I*, 6th edn., WMO-No. 168. World Meteorological Organization, Geneva. §§ 5.4, 5.7, 6.2.

[16] Efron, B. & Tibshirani, R.J. (1994). *An Introduction to the Bootstrap*. Chapman & Hall/CRC Monographs on Statistics and Applied Probability, Vol. 57. CRC Press, Boca Raton. doi:10.1201/9780429246593

[17] Scholz, F.W. & Stephens, M.A. (1987). K-sample Anderson-Darling tests. *Journal of the American Statistical Association*, 82(399), 918–924. doi:10.1080/01621459.1987.10478517

[18] Rodríguez-Iturbe, I., Cox, D.R. & Isham, V. (1987). Some models for rainfall based on stochastic point processes. *Proceedings of the Royal Society of London A*, 410(1839), 269–288. doi:10.1098/rspa.1987.0039